SUPPLEMENTARY INFORMATION

## 1. The measurement on the bulk bandgap

The bulk bandgap of the microwave photonic crystals was measured using vector network analysis through antennas A and B in a finite 16x10 crystal. The two antennas were arranged 8 lattice constants apart inside the crystal as illustrated in Fig. S-1b. The measurement was performed from 1GHz to 6GHz, covering the first three TM bandgaps (Fig. S-1a). Because of the power reflection at the edges of the finite crystal, power transmission between antennas A and B is facilitated through a number of waves with various wavevectors, which is not limited to the case of the wavevectors being parallel with the x direction. Calculated field patterns (Fig. S-1b-S-1e) indicate that the evanescent propagation between A and B with power transmission suppressed by orders of magnitude is only established in a complete bandgap (Fig. S-1c, S-1e). Therefore, it is possible to derive the frequency range of the bandgap from a single measurement as illustrated in Fig. 3a. We also note that the system has 180-degree rotational symmetry, resulting in identical power transmission for the forward and backward directions.

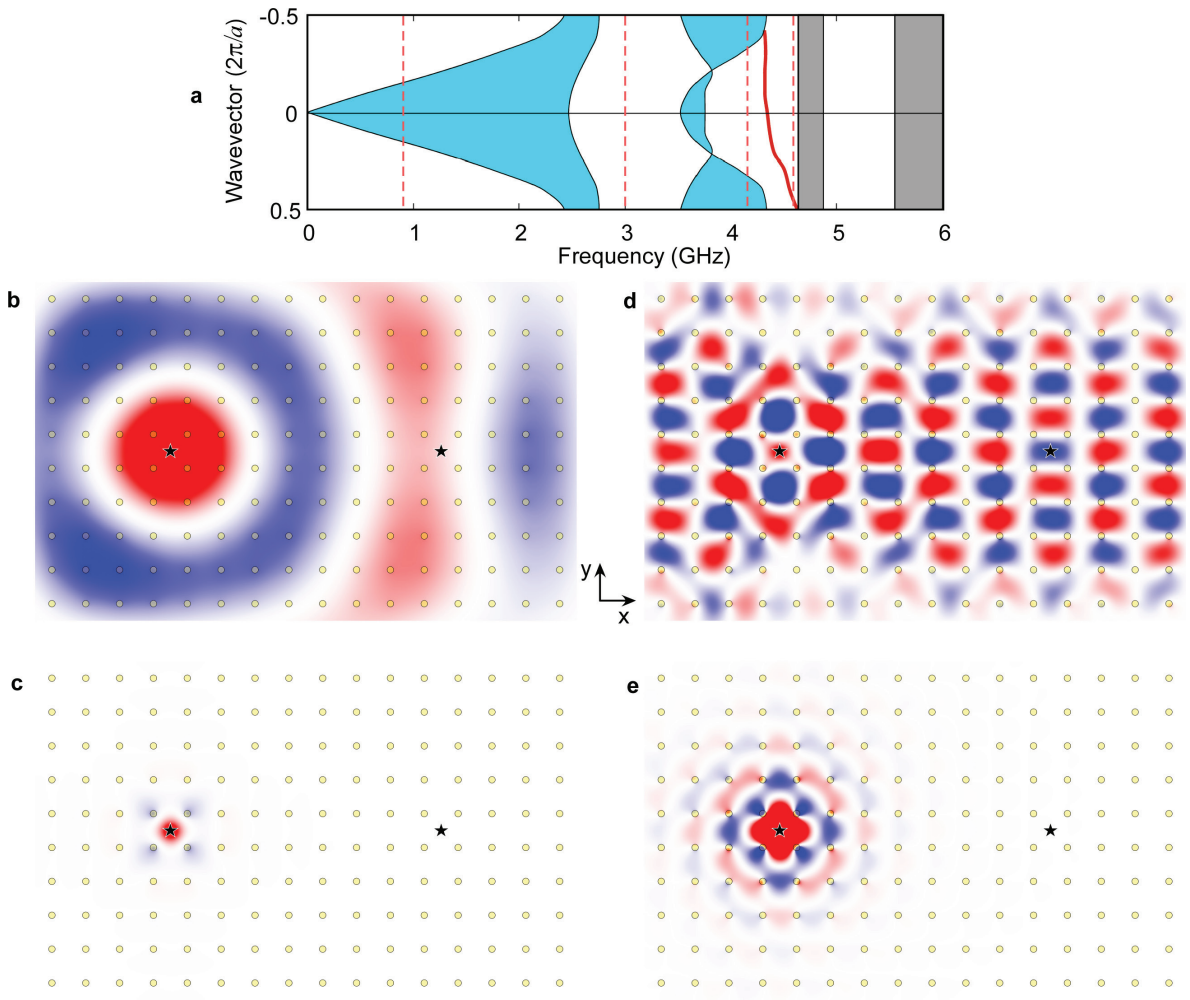


Fig. S-1. **Calculated field distributions between the probe antennas (black stars) configured to measure the bandgap of the bulk crystal**. **a**, the projected bandstructure of the bulk crystal. **b-e**, the calculated field patterns at 0.9GHz, 3.0GHz, 4.1GHz and 4.55GHz (marked as dashed lines in **a**) respectively.

## 2. The "magnetic" bandgap

The existence of one-way topological chiral edge states (CESs) is dictated by the topological Chern number of the bulk photonic bands. As explained in earlier papers, these modes reside in a bandgap opened up by external DC magnetic fields through gyrotropic response of the constituent material in the photonic crystal. In the case of microwave ferrites, the strong gyrotropic response occurs near the frequency of the ferromagnetic resonance, which in turn is controlled by the field strength of the DC magnetic bias. Such a "magnetic" bandgap supports one-way CESs at the bandgap frequencies, and its frequencies are strongly dependent on the applied magnetic bias. In contrast, a conventional photonic bandgap does not support CESs and spans a frequency range largely independent of the applied magnetic bias. To demonstrate this intrinsic link between the applied magnetic field and the frequency span of the "magnetic" bandgap, we have measured the transmission spectra of a bulk crystal under various DC magnetic biases. As shown in Fig. S-2, the frequency range of the "magnetic" bandgap (the 2$^{nd}$ bandgap) indeed shows a strongly monotonic dependence on the applied magnetic field, while a conventional bandgap with a trivial sum of the topological Chern numbers (the 1$^{st}$ bandgap) is largely unperturbed by the change in the DC magnetic bias. We also note that the "magnetic" bandgap between the second and the third TM bands does not open when the applied DC magnetic field is zero[1]. Consequently the transmission spectrum at $H_{DC} = 0$ is irrelevant to the CESs in the photonic crystal.

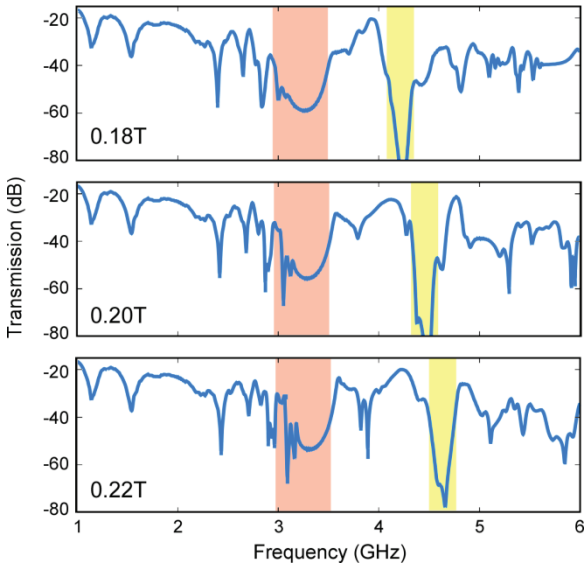


Fig. S-2. Measured transmission spectra of a bulk crystal (a16x10 array, configured identically to the setup used for Fig. 3a and S-1) show a "magnetic" bandgap (yellow) with its frequency range strongly dependent on the applied DC magnetic field. The conventional bandgap (red) is largely unaffected despite the change in the magnetic bias.

## 3. Movies: A comparison of a one-way CES waveguide and a conventional two-way waveguide

In the absence of absorption losses, when a one-way CES mode encounters a scatterer, regardless of its size, as long as the gyrotropic photonic crystal cladding is not completely penetrated, the edge mode is capable of flowing around the scatterer with complete transmission. The details of the scatterer are unimportant, since the existence of the newly-formed waveguide around the scatterer is topologically guaranteed. In stark contrast, light propagating in a conventional two-way waveguide will typically suffer a large backscattering and the amplitude of the scattering strongly depends on the size, shape and the position of the scatterer. To illustrate the difference and to show the propagation of the one-way mode over time, we animated the simulation results in Fig. 2 to show the field distributions with the phase angle being stepped through a full optical cycle. A dipole antenna radiates only along the forward (rightward) direction in a CES waveguide (Movie S1, S2), while an identical antenna radiates both ways in a two-way waveguide (Movie S3-S5). The contrast between Movie S2 and Movie S5 demonstrates the disorder-immunity of a one-way CES waveguide, even in the case of a very large scatterer that almost completely blocks the transmission in a conventional two-way waveguide. Even a scatterer of a much smaller size is sufficient to cause a great deal of backscattering in a conventional two-way waveguide (Movie S4).

Movie S1: One-way CES mode being excited by a dipole antenna, as in Fig.2a. The black circle represents the approximate location of the source.

Movie S2: One-way CES mode circumventing a scatterer with a length of 1.65 lattice constants, as in Fig.2b.

Movie S3: A conventional waveguide (with no gyrotropic materials) being excited by a dipole antenna identical to the one used in Movie S1 and Fig. 2a. The radiation occurs in both directions in this case. The high-index materials in this photonic crystal feature identical dielectric constants and dimensions to the ferrites used in Fig.2 and Movie S1 and S2. The relative permeability of the entire structure is $\mu = 1.0$. A dielectric strip with a relative permittivity of $\varepsilon = 7.0$ and a width of $0.5a$ is placed next to the metallic wall in order to support a line defect modes (two-way) at the metal/photonic-crystal interface. The spatial distribution of the unit cell function of the waveguide mode causes the fields (Ez) to appear to weaken once every half cycle. At the minimum of the electric field strength, the electromagnetic energy is stored mostly in the in-plane magnetic field (not shown). *a* is the lattice constant of the photonic crystal. The excitation frequency is 0.43 ($2\pi c/a$).

Movie S4: Adding a small metallic scatterer of the size $0.3a$(L)x$0.25a$(W) causes the majority of the right-traveling waves being reflected towards the left. A strong standing wave pattern can be seen between the source and the scatterer. *a* is the lattice constant of the photonic crystal.

Movie S5: Increasing the length of the scatterer to $1.65a$ almost completely blocks the transmission towards the right direction. The transmitted fields are four orders of magnitude smaller than the incident fields, barely observable in the linear-scale pseudo-color plot. A strong standing wave appears between the source and the scatterer.

1. Wang, Z., Chong, Y. D., Joannopoulos, J. D., & Soljacic, M., Reflection-free one-way edge modes in a gyromagnetic photonic crystal. *Phys. Rev. Lett.* **100** (1), 013905 (2008).